Author/s:
Rainczuk, AK;Klatt, S;Yamaryo-Botté, Y;Brammananth, R;McConville, MJ;Coppel, RL;Crellin, PK

Title:
Mtrp, a putative methyltransferase in corynebacteria, is required for optimal membrane transport of trehalose mycolates

Date:
2020-05-01

Citation:
Rainczuk, A. K., Klatt, S., Yamaryo-Botté, Y., Brammananth, R., McConville, M. J., Coppel, R. L. & Crellin, P. K. (2020). Mtrp, a putative methyltransferase in corynebacteria, is required for optimal membrane transport of trehalose mycolates. Journal of Biological Chemistry, 295 (18), pp.6108-6119. https://doi.org/10.1074/jbc.RA119.011688.

Persistent Link:
https://hdl.handle.net/11343/331895

JBC ARTICLE

MtrP, a putative methyltransferase in Corynebacteria, is required for optimal membrane transport of trehalose mycolates

Received for publication, October 29, 2019, and in revised form, March 22, 2020 Published, Papers in Press, March 26, 2020, DOI 10.1074/jbc.RA119.011688

Arek K. Rainczuk[‡1], Stephan Klatt[§1,2], Yoshiki Yamaryo-Botté[§3], Rajini Brammananth[‡], Malcolm J. McConville[§4], Ross L. Coppel[‡4], and Paul K. Crellin[‡4,5]

From the [‡]Infection and Immunity Program, Monash Biomedicine Discovery Institute and Department of Microbiology, Monash University, Victoria 3800, Australia and the [§]Department of Biochemistry and Molecular Biology, Bio21 Institute of Molecular Sciences and Biotechnology, University of Melbourne, Parkville, Victoria 3010, Australia

Edited by Chris Whitfield

Pathogenic bacteria of the genera *Mycobacterium* and *Corynebacterium* cause severe human diseases such as tuberculosis (*Mycobacterium tuberculosis*) and diphtheria (*Corynebacterium diphtheriae*). The cells of these species are surrounded by protective cell walls rich in long-chain mycolic acids. These fatty acids are conjugated to the disaccharide trehalose on the cytoplasmic side of the bacterial cell membrane. They are then transported across the membrane to the periplasm where they act as donors for other reactions. We have previously shown that transient acetylation of the glycolipid trehalose monohydroxycorynomycolate (hTMCM) enables its efficient transport to the periplasm in *Corynebacterium glutamicum* and that acetylation is mediated by the membrane protein TmaT. Here, we show that a putative methyltransferase, encoded at the same genetic locus as TmaT, is also required for optimal hTMCM transport. Deletion of the *C. glutamicum* gene *NCgl2764* (*Rv0224c* in *M. tuberculosis*) abolished acetyltrehalose monocorynomycolate (AcTMCM) synthesis, leading to accumulation of hTMCM in the inner membrane and delaying its conversion to trehalose dihydroxycorynomycolate (h2TDCM). Complementation with *NCgl2764* normalized turnover of hTMCM to h2TDCM. In contrast, complementation with *NCgl2764* derivatives mutated at residues essential for methyltransferase activity failed to rectify the defect, suggesting that NCgl2764/Rv0224c encodes a methyltransferase, designated here as MtrP. Comprehensive analyses of the individual *mtrP* and *tmaT* mutants and of a double mutant revealed strikingly similar changes across several lipid classes compared with WT bacteria. These findings indicate that both MtrP and TmaT have nonredundant roles in regulating AcTMCM synthesis, revealing additional complexity in the regulation of trehalose mycolate transport in the Corynebacterineae.

Bacteria of the Corynebacterineae, a suborder of the Actinomycetales, include several species pathogenic to humans, including *Mycobacterium tuberculosis*, *Mycobacterium leprae*, and *Corynebacterium diphtheriae*. The former latently infects around one-quarter of all humans (~1.7 billion) and causes active tuberculosis (TB)[6] disease that is responsible for 1.6 million deaths annually. In 2017, around 10 million people developed TB, mostly in sub-Saharan Africa and Asia. Drug resistance is a significant problem, with ~0.6 million people developing rifampicin-resistant TB in 2017, 82% of which were multidrug-resistant TB (1). The unusually hydrophobic and distinctive cell wall of these bacteria is a validated drug target, and several first line TB drugs, such as isoniazid and ethambutol, target cell wall biosynthetic pathways. An improved understanding of cell wall synthesis processes is required to reveal and exploit new targets.

The Corynebacterineae cell wall confers intrinsic resistance to antibiotics and host immune responses (2, 3). The inner layers comprise peptidoglycan and arabinogalactan (AG) as well as covalently-linked very-long-chain fatty acids, the mycolic acids, that form the bulk of an outer membrane (4). These α-alkyl β-hydroxyl fatty acids (70–90 carbons long) are either linked to terminal arabinose residues of the AG polymer or are present as free lipids esterified to trehalose (trehalose monomycolate

This work was supported by National Health and Medical Research Council of Australia Project Grant 1064466 (to P. K. C., R. L. C., and M. J. M.), Australian Research Council Centre of Excellence in Structural and Functional Microbial Genomics Grant COE562063 (to R. L. C.), and Australian Research Council Discovery Grant 180102463 (to R. L. C. and M. J. M.). The authors declare that they have no conflicts of interest with the contents of this article.

This article contains Figs. S1–S6.

[1] Both authors contributed equally as first authors.

[2] Present address: The Florey Institute of Neuroscience and Mental Health, Melbourne Dementia Research Centre, University of Melbourne, 30 Royal Parade, Parkville, Victoria 3052, Australia.

[3] Present address: ApicoLipid Team, Institute for Advanced Biosciences, Université Grenoble Alpes, CNRS UMR5309, INSERM U1209, Grenoble, France.

[4] These authors contributed equally as senior authors.

[5] To whom correspondence should be addressed: Infection and Immunity Program, Monash Biomedicine Discovery Institute and Dept. of Microbiology, Monash University, Victoria 3800, Australia. Tel.: 61-3-9902-9148; E-mail: paul.crellin@monash.edu.

[6] The abbreviations used are: TB, tuberculosis; hTMCM, trehalose monohydroxycorynomycolate; h2TDCM, trehalose dihydroxycorynomycolate; AcTMCM, acetyltrehalose monocorynomycolate; ketoTMCM, monoketocorynomycolate; TMM, trehalose monomycolate; TDM, trehalose dimycolate; GMM, glucose monomycolate; TmaT, TMCM mycolyl acetyltransferase; AG, arabinogalactan; LAM, lipoarabinomannan; LM, lipomannan; HPTLC, high-performance thin-layer chromatography; ZOI, zone of inhibition; PG, phosphatidylglycerol; CL, cardiolipin; SAM, *S*-adenosylmethionine; Gl-X, mannosyl-glucuronic acid diacylglycerol; AcPIM2, Man_2-acyl-PI; IM, inner membrane; OM, outer membrane; Ala-DAG, alanylated diacylglycerol; BHI, brain heart infusion; PI, phosphatidylinositol.

(TMM) and trehalose dimycolate (TDM)), glucose (GMM), or glycerol (5, 6). The Corynebacteria also synthesize mycolic acids, the corynomycolates, that are shorter (C_{22} to C_{36}) and structurally less complex than the mycobacterial fatty acids (7).

The synthetic pathways and enzymatic machineries that produce these species have been extensively studied and reviewed (4, 8–11). In Mycobacteria, two independently-synthesized fatty acids, the short α branch (C_{24}–C_{26}) and long meromycolate chain (C_{50}–C_{60}), produced by the single FAS-I enzyme and FAS-II complex (12, 13), respectively, are modified and then condensed by the cytoplasmic polyketide synthase, Pks13 (14), to form a 2-alkyl 3-keto fatty acid that is then reduced by CmrA to generate the mature, hydroxylated mycolic acid (15). These fatty acids are conjugated to trehalose to form TMM, which is then bound and flipped to the periplasm by the integral membrane lipid transporter MmpL3 (16, 17), the target of several classes of new antimycobacterial inhibitors (18, 19). Whereas structurally-diverse classes of MmpL3 inhibitors have been reported, several of these compounds were subsequently found to indirectly inhibit MmpL3 by disrupting the transmembrane electrochemical proton gradient (20). However, recent studies have identified two compounds, BM212 (a 1,5-diarylpyrrole compound) and PIPD1 (a piperidinol-containing molecule), that inhibit MmpL3 via direct interactions, advancing our understanding of the mechanism of action of this transporter (16, 21). Periplasmic mycolyltransferases of the Ag85ABC complex (22) subsequently utilize TMM in the periplasmic space as the mycolic acid donor for the synthesis of the mycolated-AG layer, trehalose dimycolate (TDM), or mycolated glucose or glycerol.

Most cell wall components are essential for the growth of pathogenic mycobacteria, hampering efforts to functionally characterize genes involved in cell wall assembly. In contrast, Corynebacteria such as *Corynebacterium glutamicum* retain viability after loss of conserved cell wall components and are thus excellent model systems for investigating cell wall synthesis in Corynebacterineae (15, 23–28). Recently, we identified a new trehalose monocorynomycolate (TMCM) glycolipid species in *C. glutamicum*, which contains an acetyl group on the corynomycolate chain. This species, termed acetyl-trehalose monocorynomycolate (AcTMCM), required expression of the putative acetyltransferase, TmaT (NCgl2759) (Fig. 1). Genetic deletion of *tmaT* significantly reduced the rate of corynomycolate transport across the inner membrane and subsequent conversion to h2TDCM, indicating that AcTMCM is the major substrate transported by *C. glutamicum* CmpL1/4 (NCgl0228/NCgl2769) (Fig. 1) (28).

Here, we show that optimal transport of hTMCM is also regulated by a methyltransferase. Specifically, we show that disruption of a putative methyltransferase gene, *NCgl2764*, which is located in the *tmaT* locus, also leads to the accumulation of hTMCM on the cytoplasmic site of the inner membrane and defects in the synthesis of h2TDCM. Comprehensive lipidomic analysis of WT and mutant *C. glutamicum* (29) suggested that NCgl2764 is required for synthesis of AcTMCM. The mutant also accumulated trehalose monoketocorynomycolates (ketoTMCM), had supressed synthesis of phosphatidylglycerol (PG), and alanylated diacylglycerols (Ala-DAG), and lacked a class of acyl-PG–like lipids, mirroring the general lipid phenotype of a *tmaT* mutant. Mutation analysis provided further support for NCgl2764 having methyltransferase activity, revealing unexpected complexity in the regulation of corynomycolate transport across the inner membrane of these bacteria.

Results

Identification of the corynebacterial ortholog of M. tuberculosis Rv0224c

We have previously identified a genetic locus in *C. glutamicum* that harbors a number of genes involved in regulating cell wall synthesis. This locus is conserved in all Corynebacterineae (15, 25, 30) and contains *NCgl2759* (*tmaT*, *Rv0228*) (28), *NCgl2760* (*Rv0227c*) (31), and *NCgl2764* (*Rv0224c*) (Fig. 2). *NCgl2764* is functionally uncharacterized but is predicted to encode a protein of 257 residues, sharing 49% identity and 86% similarity with *M. tuberculosis* Rv0224c (Fig. S1). NCgl2764/Rv0224c is annotated as a cytoplasmic methyltransferase based on weak similarity with a range of methyltransferases and the presence of conserved residues essential for activity (see below).

Loss of the NCgl2764 gene affects growth of C. glutamicum

To investigate the function of this gene/protein, a two-step recombination strategy was used to create the *NCgl2764* mutant (Fig. 3). Sequences flanking the gene were PCR-amplified and cloned into the suicide vector pK18*mobsacB* (32), which carries a kanamycin resistance gene (*aph*) and *Bacillus subtilis sacB* gene conferring sensitivity to sucrose. This plasmid was introduced into *C. glutamicum* 13032, and a *NCgl2764* deletion mutant, designated Δ*NCgl2764,* was isolated, and gene deletion was confirmed by PCR analysis (Fig. 3, *A* and *B*). The Δ*NCgl2764* mutant formed small colonies relative to the wild-type (WT) parent on agar plates and displayed an extended lag-phase in liquid BHI medium, although it ultimately achieved a final cell density comparable with the WT parent strain (Fig. 3*C*). A similar growth phenotype was observed following loss of *tmaT* (*i.e.* Δ*NCgl2759*) but not other genes (*i.e.* Δ*NCgl2760*) in this locus (28, 31).

Complementation of C. glutamicum ΔNCgl2764

Complementation and control strains were created to determine whether the growth defect was due solely to disruption of *NCgl2764*. To complement the mutant, Δ*NCgl2764* was transformed with pSM22:*NCgl2764*, a plasmid carrying a full-length *NCgl2764* gene plus 203 bp of upstream sequence. The empty pSM22 vector (32) was also introduced into Δ*NCgl2764* as a control. Growth curves indicated that introduction of pSM22:*NCgl2764* into the Δ*NCgl2764* mutant restored normal lag phase and growth, whereas the empty pSM22 vector did not (Fig. 3*C*).

Antibiotic susceptibility testing

Corynebacterial mutants with defects in cell wall synthesis and integrity characteristically display increased sensitivity to antibiotics. To test the condition and permeability of the cell wall in the Δ*NCgl2764* mutant, the strains were cultured on agar media and exposed to paper discs impregnated with a vari-

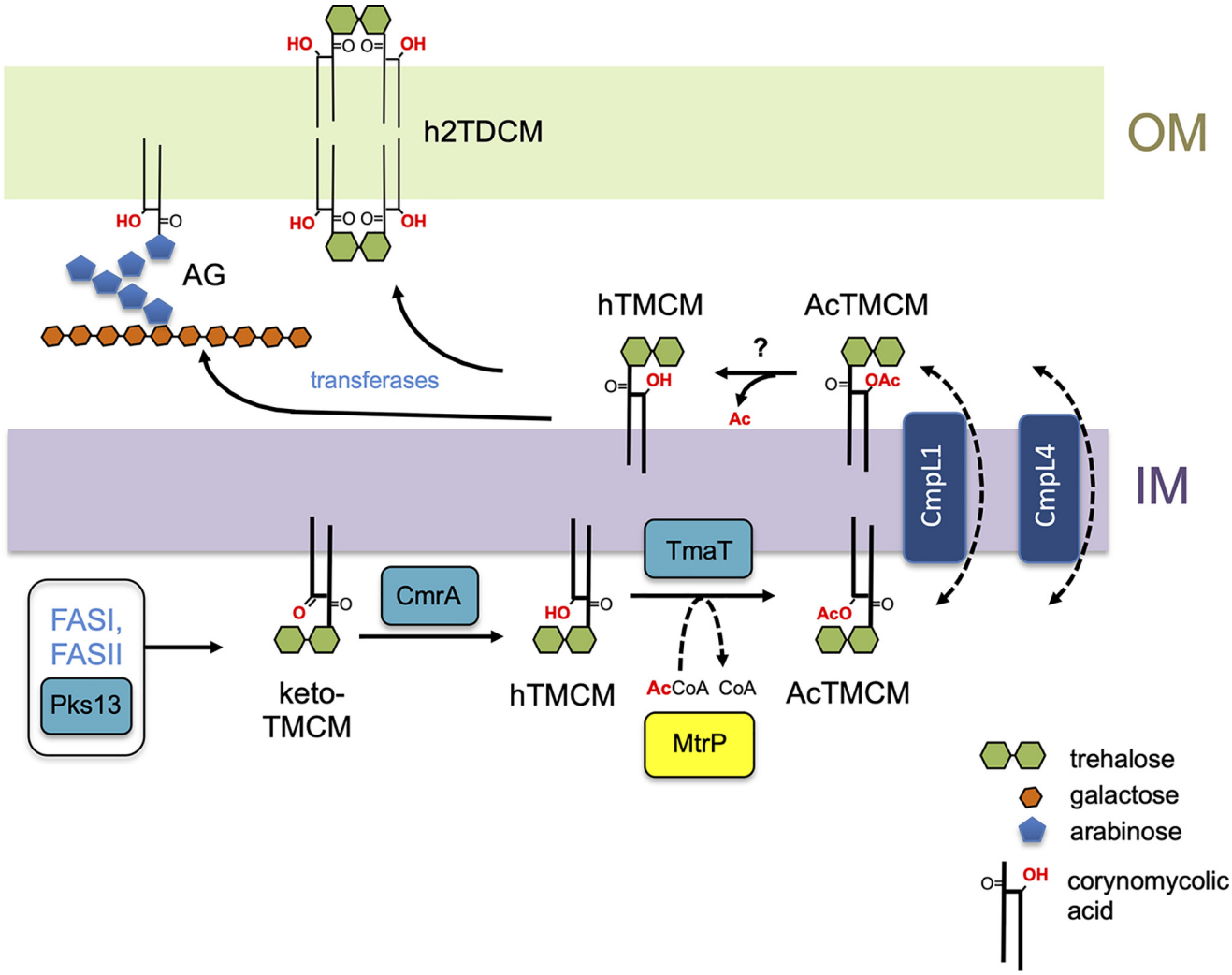

Figure 1. Pathway of trehalose corynomycolate synthesis and transport in *C. glutamicum*. Products of the FAS-I and FAS-II pathways are condensed and then attached to trehalose, producing keto-TMCM in the inner leaflet of the IM. Reduction by CmrA produces hTMCM, which may be acetylated to AcTMCM by the integral membrane acetyltransferase TmaT, facilitating transport by CmpL1/4. It is hypothesized that an unidentified deacetylase removes the acetyl group after transport, reconstituting hTMCM in the outer leaflet of the IM. Trehalose corynomycolyl transferase then produce h2TDCM from two hTMCM molecules or transfer the corynomycolates to acceptors on AG. Other acylation variants of hTMCM, AcTMCM, and hTDCM have been identified (29) but are not shown here for clarity. Results of this study place NCgl2764 (MtrP) at the same step as TmaT in the pathway.

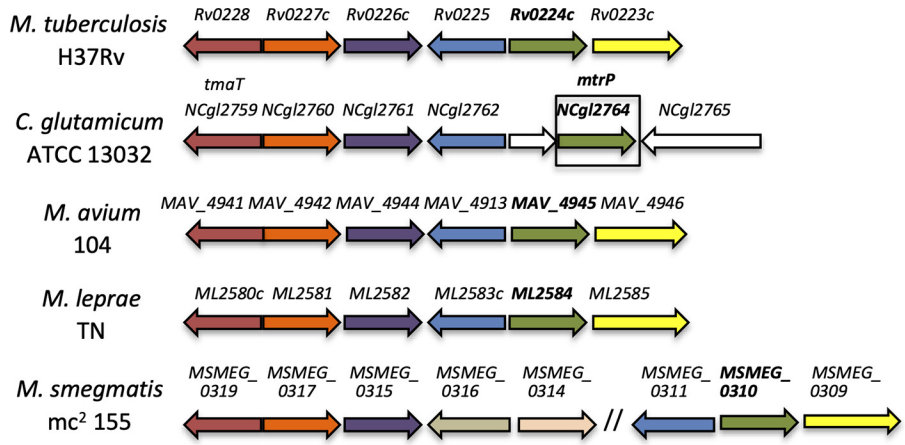

Figure 2. NCgl2764 is encoded within a genetic locus highly conserved in Corynebacterineae. The *tmaT* locus of Corynebacterineae is shown. Likely ortholog genes in the four species are shown using the same color. The focus of this study *NCgl2764* (*boxed*) and its likely mycobacterial orthologs are shown in *bold*. *MSMEG_0310* is reported to be a pseudogene. Previously studied genes are *NCgl2759* (*tmaT* (28)) and *NCgl2760* (31), whereas the remaining genes remain uncharacterized.

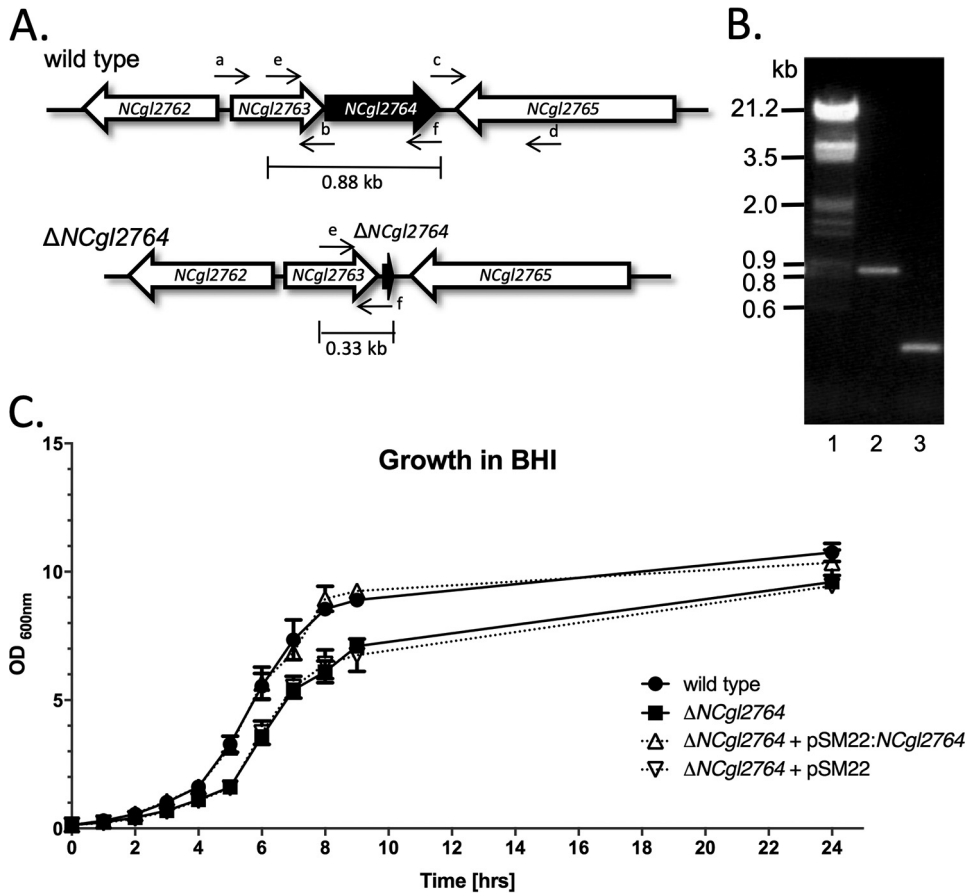

Figure 3. Disruption strategy and growth analysis for the Δ*NCgl2764* mutant. *A,* diagram showing the arrangement of genes in the *NCgl2764* region of WT *C. glutamicum* (*above*) and Δ*NCgl2764* mutant (*below*). *Small horizontal arrows* indicate the binding sites for the four primers used to construct the Δ*NCgl2761* mutant (*arrow a*, NCgl2764leftfor; *arrow b*, NCgl2764leftrev; *arrow c*, NCgl2764leftrightfor; *arrow d*, NCgl2764rightrev) and screen for the gene knockout (*arrow e*, NCgl2764-comp_F; *arrow f*, NCgl2764-comp_R). Expected PCR product sizes using the *e/f* primer combination are indicated in kb (kilobase pairs). *B,* PCR amplification of genomic DNA of *C. glutamicum* WT (*lane 2*) and the Δ*NCgl2764* mutant (*lane 3*) using primers *e* and *f*. Positions of the Sigma-Aldrich DNA markers III (*lane 1*) are indicated in kb. *C,* growth curves of WT *C. glutamicum*, the Δ*NCgl2764* mutant, and complementation strains in liquid BHI medium. Each strain was grown to saturation and then diluted 1:100 in fresh BHI medium. Triplicate cultures were sampled at the times indicated to determine the optical density (*OD*) at a wavelength of 600 nm. The *curves* for the WT and Δ*NCgl2764* + pSM22:*NCgl2764* (complementation) strains overlap, as do the Δ*NCgl2764* and Δ*NCgl2764* + empty pSM22 strains, indicating that adding back the *NCgl2764* gene reverses the mild growth defect in the mutant.

ety of antibiotics. The sensitivity of the strains was assessed by the size of zones of inhibition (ZOI) around the discs. For low-molecular-weight antibiotics (<500 g/mol), the Δ*NCgl2764* mutant displayed significantly larger ZOIs than the WT parent ($p < 0.05$) and complemented strains (Fig. 4). The increases in zone diameter were particularly apparent for the β-lactam class antibiotics amoxicillin, cefoxitin, and imipenem, suggesting increased access of the drugs to the peptidoglycan layer. Increased sensitivity to drugs targeting cytoplasmic processes (RNA and protein synthesis) was also observed. Clustering of the *NCgl2764* gene with cell wall biosynthesis genes, together with the altered growth rate and increased antibiotic sensitivity in the Δ*NCgl2764* strain, suggested a role for the encoded protein in cell wall biosynthesis.

Loss of NCgl2764 affects synthesis of trehalose corynomycolates

HPTLC analysis of lipid extracts of WT and Δ*NCgl2764* bacteria revealed major differences in the abundance of several different cell wall lipid classes (Fig. 5*A*). In particular, the Δ*NCgl2764* mutant accumulated a lipid species during logarithmic growth (15, 28) that comigrated with hTMCM on HPTLC and was confirmed to be this glycolipid by MALDI-TOF–MS (Fig. S2). The accumulation of hTMCM in Δ*NCgl2764* was associated with a concomitant decrease in levels of h2TDCM, relative to WT (Fig. 5*A*). Levels of both species were restored following complementation of the mutant with pSM22:*NCgl2764*, but not with empty pSM22. These data suggest that NCgl2764 is required for efficient conversion of hTMCM to h2TDCM.

To determine whether the *M. tuberculosis* ortholog, Rv0224c, could functionally complement the mutant, we constructed a pSM22:*Rv0224c* plasmid and introduced it into the Δ*NCgl2764* mutant. hTMCM and h2TDCM levels in the Rv0224c complemented line were unchanged compared with the original mutant (Fig. S3), suggesting that Rv0224c is unable to substitute for NCgl2764. Although the two proteins share significant sequence similarity, including two glycine residues essential for methyltransferase function (see below and Fig. S1), the Rv0224c homolog may lack sequence motifs required for protein–protein interactions essential for activity in *C. glutamicum*.

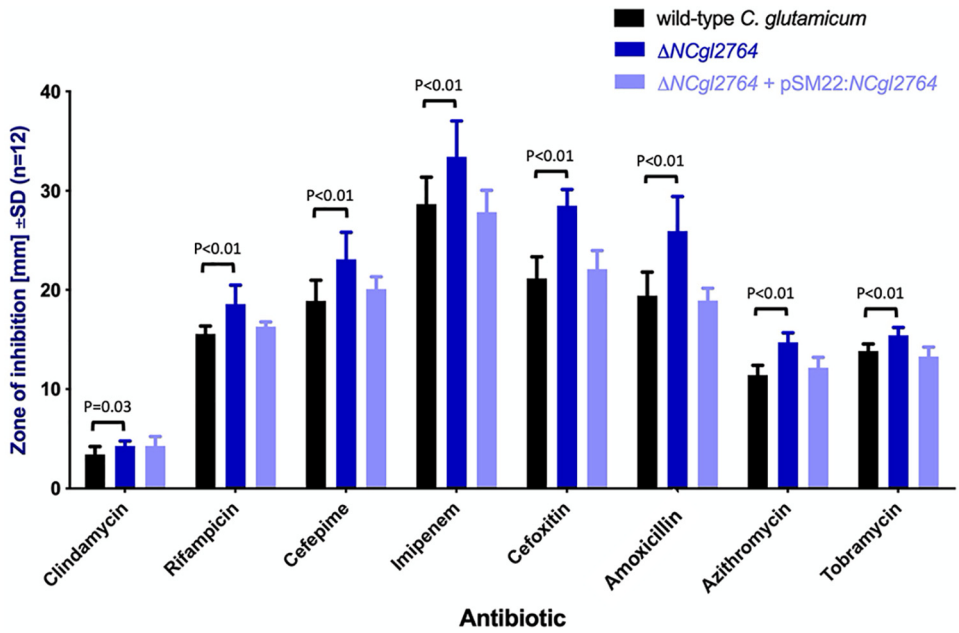

Figure 4. Antibiotic susceptibility of a *C. glutamicum* Δ*NCgl2764* mutant. Antibiotic sensitivity was measured by determining the ZOI around antibiotic-soaked discs placed on BHI plates spread with the indicated strains.

Labeling studies

To measure rates of glycolipid turnover in WT and mutant lines, bacteria were pulse-labeled with [^{14}C]acetate, then suspended in BHI medium (chase), and sampled at various time points. Cell wall lipids were then separated by HPTLC, and labeled species were detected by autoradiography (Fig. 5*B*). Label was rapidly incorporated into hTMCM and phosphatidylglycerol (PG) species during the pulse and subsequently into h2TDCM in the 5-min chase in WT cells. In contrast, the label was not incorporated into h2TDCM in the Δ*NCgl2764* strain throughout the 60-min chase period, demonstrating a significant delay in its synthesis. Interestingly, in contrast to the orcinol-stained samples (Fig. 5*A*), no accumulation of [^{14}C]hTMCM was observed in the Δ*NCgl2764* mutant, implying that the high steady-state levels of hTMCM (Fig. 5*A*) reflect reduced rate of turnover of hTMCM rather than excess production of this glycolipid. Interestingly, incorporation of ^{14}C-label into PG lipids was also reduced in the Δ*NCgl2764* mutant, similar to the phenotype of the *tmaT* mutant (29) and consistent with the lipidomics analysis (see below).

Altered dynamics of hTMCM turnover and h2TDCM synthesis in a ΔNCgl2764 mutant

To investigate the dynamics of hTMCM conversion to h2TDCM in the mutant, glycolipids were extracted at specific growth stages and analyzed by HPTLC. Cells were cultured in BHI and sampled at OD_{600} 0.5–10 after 24 h (stationary phase). Samples were extracted and normalized by pellet wet weight prior to HPTLC analysis (Fig. 5*C*). In the WT and complemented Δ*NCgl2764* mutant, h2TDCM levels steadily increased from early log phase through to the stationary phase, peaking by OD_{600} ~4. hTMCM levels also peaked at OD_{600} ~4 and then reduced to be undetectable by stationary phase. In the Δ*NCgl2764* mutant, an accumulation of hTMCM was observed by OD_{600} ~2 (early log phase) before reducing at OD_{600} ~7, and these species were still detectable in stationary phase. h2TDCM synthesis was delayed in the mutant, not reaching maximal levels until OD_{600} ~7. These findings suggested that synthesis of h2TDCM from hTMCM is delayed in the Δ*NCgl2764* strain, consistent with a defect in the rate of transport of hTMCM to the periplasmic space in logarithmic phase.

Because hTMCM is known to be the donor of corynomycolates for formation of the AG-linked corynomycolate outer membrane, we also extracted and analyzed covalently-bound corynomycolates from the delipidated pellets. No significant differences were observed between WT and the mutant at the various time points (Fig. S4), suggesting that the limited pool of transported corynomycolates are channeled to AG at the expense of h2TDCM synthesis. Unaltered levels of AG-linked corynomycolates were also observed in a *tmaT* mutant (28).

Global changes in the cell envelope composition in the C. glutamicum NCgl2764 mutant

To further investigate whether hTMCM does indeed accumulate on the cytoplasmic leaflet of the IM in the Δ*NCgl2764* mutant, IM and OM lipid extracts of the WT and mutant strains were analyzed by LC–ESI–QTOF-MS in a positive ionization mode (29). Lipid species identified by MS/MS from WT and the Δ*NCgl2764* mutant are shown in Table 1. After removal of isotopologs, dimer species, isomers, and isobars, 139 and 111 lipid species were identified with high confidence in the IM and OM of the *NCgl2764* mutant, respectively. Compared with WT bacteria, the IM fraction of the *NCgl2764* mutant contained elevated levels of hTMCM, ketoTMCM, and hGMM species. Conversely, levels of PG and Ala-DAG species were decreased, whereas AcTMCM and acyl-PG like species were either absent or present at very low levels. These changes were also observed in the *tmaT* (*NCgl2759*) mutant lipidome (Table 1) (29).

As *NCgl2764* encodes a putative methyltransferase, we looked for evidence that major TMCM species might be meth-

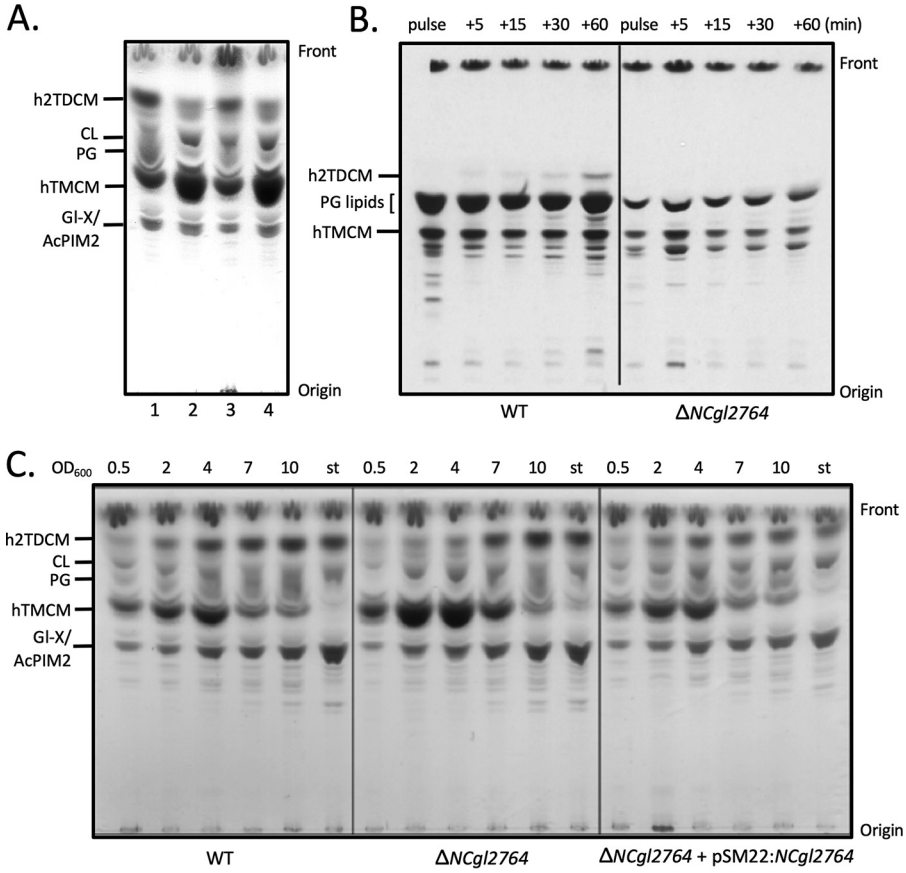

Figure 5. Altered lipid composition and dynamics of turnover in a *C. glutamicum* Δ*NCgl2764* mutant. *A,* Δ*NCgl2764* mutant accumulates hTMCM during active growth. HPTLC analyses of cell wall glycolipids extracted and purified from cells growing in logarithmic phase (OD_{600} = 3) are shown. Lipids were separated by HPTLC and then visualized by orcinol-sulfuric acid staining the following: *lane 1*, WT; *lane 2*, Δ*NCgl2764* mutant; *lane 3*, Δ*NCgl2764* containing pSM22:*NCgl2764*; *lane 4*, Δ*NCgl2764* containing empty pSM22. *B,* pulse/chase labeling reveals delayed synthesis of h2TDCM in a Δ*NCgl2764* mutant. Autoradiogram of HPTLC analysis of [^{14}C]acetate-labeled lipids extracted during a pulse/chase experiment. The experiment reveals the dynamics of *de novo* synthesis of hTMCM/h2TDCM. In WT *C. glutamicum*, the label appears in h2TDCM within 5 min post-labeling. In contrast, no labeled h2TDCM was detected in the Δ*NCgl2764* samples even after 60 min, consistent with a significantly slower rate of h2TDCM synthesis in this strain. *C,* delayed conversion of hTMCM to h2TDCM in a Δ*NCgl2764* mutant. Glycolipids were extracted from cells harvested at OD_{600} of 0.5, 2, 4, 7, and 10 and from a stationary phase culture (~24 h growth). HPTLC analysis of glycolipids showed that the accumulation of hTMCM peaks during mid-log growth phase in the analyzed strains. In samples from the Δ*NCgl2764* strain, hTMCMs accumulate to a higher level and do so earlier than in the WT or the complemented mutant. The dynamics of h2TDCM synthesis are inverted relative to hTMCM and reach their highest point in the stationary phase where no hTMCM is detected. The identities of glycolipids were based on previously published reports. *Gl-X,* mannosyl-glucuronic acid diacylglycerol; *AcPIM2*, Man_2-acyl-PI.

ylated. Methylation of either the lipid or glycan moieties of the major TMCM species carrying C32:0, C34:0, C32:1, C34:2, C26:1 and C28:1 corynomycolic acids would increase their size by 14 Da. Methylation of the glycan headgroup would result in fragment ions corresponding to loss of 211 Da (methylated hexose with NH_4^+) and 373 Da (two hexoses with one being methylated, with NH_4^+), respectively, instead of 197 and 359 Da. However, neither of these molecular or fragment ions were detected, suggesting that TMCM is not directly methylated or that only a very small proportion of the steady-state pool of TMCM carries this modification. Changes in the relative abundance of individual lipid molecular species in WT and mutant lines were verified by quantitation of the relative ion (lipid) intensities within four replicate samples of each line. Lipids identified in the MS1 analysis are summarized in Fig. 6, *A–F*. Both MS1 and MS/MS results confirm the global lipidome changes and an overall shared phenotype between the *NCgl2764* and *tmaT* (29) mutants.

Collectively, these findings suggest that NCgl2764 is required, together with TmaT, for the synthesis of AcTMCM. To investigate whether these genes may function at the same step, we constructed a double mutant by deleting the *NCgl2764* gene in the *tmaT* mutant. The resultant strain grew similarly to the individual mutants (data not shown), and analysis of cell wall glycolipids by HPTLC with orcinol staining revealed an identical lipid profile to the individual *NCgl2764* and *NCgl2759* knockout lines (Fig. 7, *lane 6*). Specifically, the double mutant exhibited a significant accumulation of hTMCM at the expense of h2TDCM and reduced synthesis of PG lipids. These data strongly suggest that NCgl2764 and TmaT regulate the same step or pathway in these bacteria.

Lipoglycan analysis of a NCgl2764 mutant

Our previous studies on genes of this locus revealed that one of them, *NCgl2760*, was involved in lipoglycan biosynthesis (31). To determine whether loss of *NCgl2764* also impacts the synthesis of other cell wall components, lipomannan (LM) and lipoarabinomannan (LAM) were extracted from delipidated cell pellets and analyzed by PAGE and LC–TOF-MS. PAGE analysis suggested that the overall abundance and degree of

Table 1
Detected lipid (sub)classes and lipid species of the IM and OM fraction of the *C. glutamicum* WT, *tmaT* (*NCgl2759*), and *NCgl2764* mutants via LC-MS/MS ESI TOF in positive ionization mode (CE30)

	Lipid (sub) class	Wildtype		Δ*NCgl2759*		Δ*NCgl2764*	
		IM	OM	IM	OM	IM	OM
1	hTMCM	18	20	26	15	23	18
2	AcTMCM	3	8	0	0	0	0
3	keto-TMCM	3	0	10	3	8	5
4	Acyl-hTMCM	7	5	12	5	9	7
5	Acyl-AcTMCM	1	0	0	0	0	0
6	h2TDCM	28	28	30	25	27	29
7	Ac1-hTDCM	3	3	3	1	0	0
8	hGMM	5	11	8	7	8	8
9	DAG	7	4	8	4	7	5
10	Ala-DAG	11	5	9	2	7	1
11	CDP-DAG	1	0	1	0	1	1
12	TAG	10	10	11	11	11	10
13	PG	11	5	5	2	6	5
14	Acyl-PG	3	0	1	0	1	0
15	Ala-PG	2	1	1	0	1	1
16	PA	2	0	0	0	1	1
17	CL	16	3	14	4	10	5
18	PI	4	3	3	2	4	5
19	PIM1	1	1	1	0	1	1
20	PIM2	1	1	1	1	1	1
21	AcPIM2	4	1	5	1	4	1
22	AcPIM3	1	0	1	0	1	1
23	AcPIM4	1	0	1	0	1	0
24	Gl-A	6	2	5	1	3	2
25	Gl-X	6	1	4	1	3	2
26	Gl-Y	1	0	1	1	0	1
27	Gl-Z	1	0	1	0	1	1
28	Acyl-PG-like	4	3	0	0	0	0
	Total	**161**	**115**	**162**	**86**	**139**	**111**

heterogeneity of these lipoglycans were similar in both the WT and Δ*NCgl2764* mutant (Fig. S5). Similarly, LC–ESI–TOF-MS analysis using a newly-developed profiling method also indicated minimal change in the LM/LAM structure in WT and the Δ*NCgl2764* mutant bacteria. The latter approach allows detection of LM and LAM molecular species that have been assembled on different lipid anchors. In WT bacteria, the glycan chains of detected LM species contain between 1 and 38 mannose residues, and six different lipid anchors, comprising PI with 2–3 acyl chains (53 molecular species total, 998 – 6997 Da after deconvolution; Fig. S6). Similarly, the LM from the Δ*NCgl2764* mutant contained between 1 and 44 mannose residues and six lipid anchors (61 molecular species, 998 and 8002 Da). Minor differences were observed between WT and mutant bacteria in the degree of polymerization of one of the lipid anchor platforms. The plots in Fig. S6 show the masses (*m*/*z*, after deconvolution) of all detected LM/LAM species, from low to high molecular weight, and the predicted mannan chain length. Fig. S5 of our previous study (31) explains, step by step, the development of Fig. S6.

Mutagenesis of NCgl2764

To investigate whether the putative methyltransferase activity of NCgl2764/Rv0224c is functionally important, the Δ*NCgl2764* mutant was complemented with plasmids encoding NCgl2764 proteins in which specific amino acids in the methyltransferase catalytic site had been mutated. The amino acid sequences of NCgl2764 and its mycobacterial orthologs were compared with two confirmed methyltransferases, MT0146/CbiT and protein arginine methyltransferase 1 (PRMT1 (33)), for which crystal structures have been solved and active-site residues identified (34, 35). Two glycine residues are conserved in nearly all analyzed *S*-adenosylmethionine (SAM)-dependent methyltransferase sequences and are known to be involved in methyl donor binding (35). These correspond to Gly-69 and Gly-71 in NCgl2764, which are also conserved in Rv0224c and ML2584 (Fig. S1). We hypothesized that substitution of either of those crucial glycine residues with alanine would result in loss of a methyltransferase function, if present, and failure to complement the Δ*NCgl2764* phenotype.

The desired mutations were engineered into the pSM22:*NCgl2764* plasmid previously used to complement the Δ*NCgl2764* strain (see above). Transformation of the deletion mutant with the pSM22:*NCgl2764*_G69A or pSM22:*NCgl2764*_G71A constructs, but not the unmodified pSM22:*NCgl2764* plasmid encoding the native protein, resulted in strains with the delayed growth phenotype (data not shown) and with glycolipid profiles identical to Δ*NCgl2764* (Fig. 7, *lanes 1–5*). This finding is in agreement with the annotation of NCgl2764 as a methyltransferase, although we cannot discount the possibility that NCgl2764 may have other functions.

Discussion

We have previously identified a conserved gene locus in mycobacteria and corynebacteria that is required for cell wall assembly (28, 29, 31). Most of the genes in this locus are essential in *M. tuberculosis*, hampering their functional characterization in this pathogen (36, 37). In contrast, these genes are not essential in *C. glutamicum*, reflecting the capacity of this bacterium to tolerate major defects in cell wall synthesis. One of the first genes characterized in this locus, *C. glutamicum NCgl2759* (ortholog of *M. tuberculosis Rv0228*, designated *tmaT*), encodes an acetyltransferase that acetylates the mycolic acid moiety of hTMCM, facilitating transport of this glycolipid across the inner membrane (28), presumptively by the MmpL3 transporter. Consistent with these findings, TmaT was recently found to be the only protein of the mycolic acid pathway to interact with MmpL3 in a two-hybrid screen (38). It remains unclear whether acetylation is required for recruitment of AcTMCM to the membrane domains containing the transporter and/or for transporter recognition and transmembrane movement. The next gene in this locus, *NCgl2760* (*Rv0227c*), has been shown to be required for synthesis of mature cell wall lipoglycans LM and LAM (31), and surprisingly, Rv0227c also interacts with MmpL3 (38). Although LM/LAM biosynthesis lacks any shared enzymes with the hTMCM pathway, both pathways are likely to be coordinately regulated to ensure balanced synthesis of major cell wall components.

In this study, we show that *NCgl2764* is also involved in cell wall synthesis. The encoded protein, denoted MtrP, shows similarity to protein methyltransferases. Phenotypic characterization of the Δ*NCgl2764* deletion mutant indicated that this protein is involved in trehalose corynomycolate metabolism, rather than LM/LAM synthesis. The mutant was found to share striking cell wall similarities with the Δ*tmaT* mutant previously characterized by our group. Both mutants failed to produce AcTMCM, accumulated hTMCM, and ketoTMCM in the IM fraction and exhibited markedly reduced kinetics of synthesis of h2TDCM (28). This phenotype is consistent with reduced

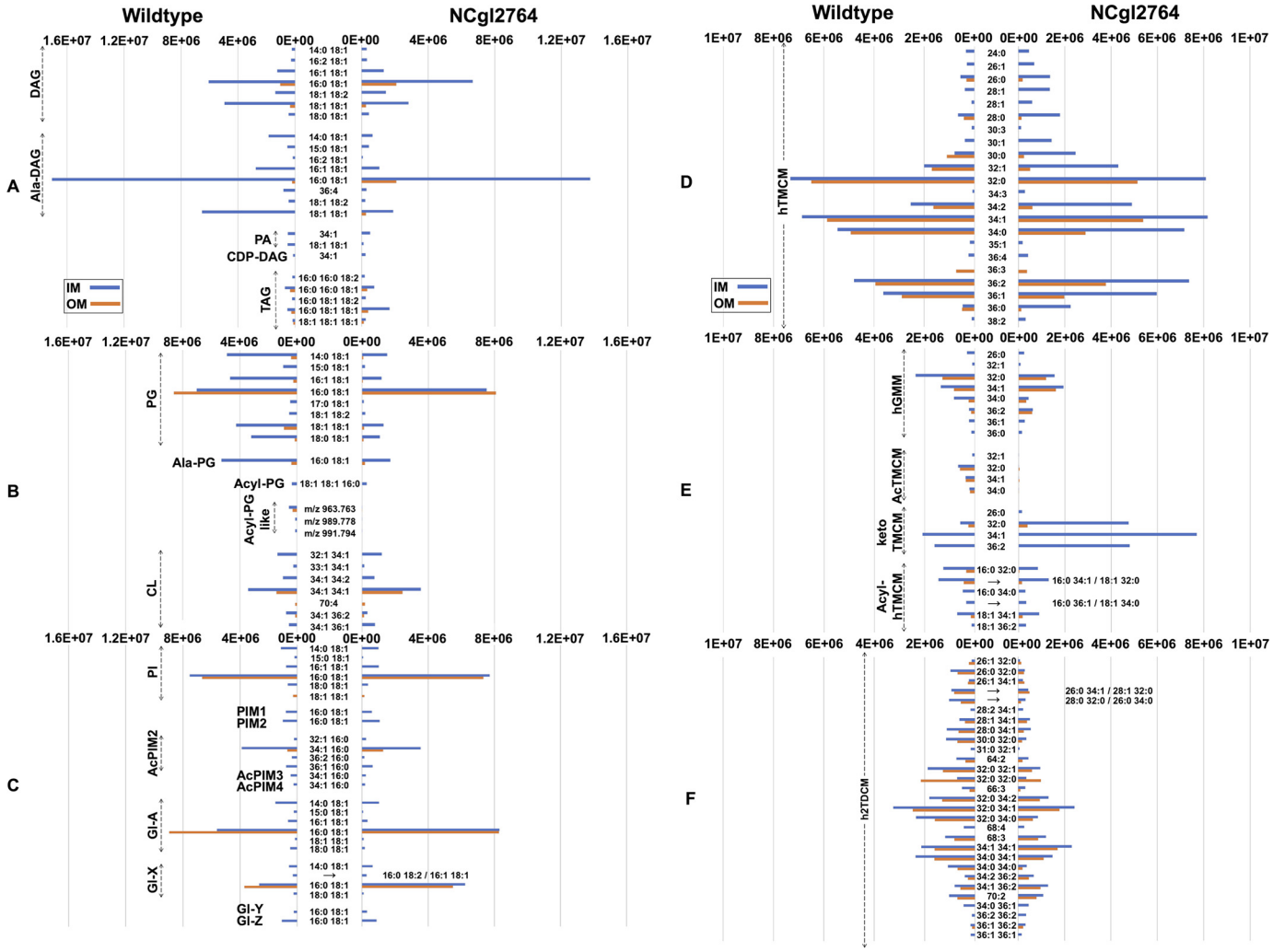

Figure 6. Comparison of the relative abundances of IM and OM lipids in *C. glutamicum* WT and the *NCgl2764* mutant. The relative abundance of 142 species, identified by LC-MS/MS profiling, in the IM and OM fractions is shown. Lipid abundances (based on ion intensities) represent the mean value of four replicates. The relative abundance of DAG- and TAG-based lipid classes (*A*), PG- and CL-based lipid classes (*B*), PI/PIM and GI glycolipid classes (*C*), hTMCM species (*D*), other trehalose and glucose corynomycolates (*E*), and h2TDCM species (*F*) are shown. Compared with WT bacteria (*left*), the IM fraction of the *NCgl2764* mutant (*right*) lacked detectable AcTMCM and acyl-PG–like species and had decreased amounts of PG, acyl-PG, Ala-DAG, and h2TDCM, whereas the OM fraction was deficient in Acyl-PG, decreased in PG, hTMCM, AcTMCM, and h2TDCM, and increased in hGMM. The lipid phenotype of the *NCgl2764* mutant shares the same major defects with a *tmaT* mutant.

transport of hTMCM across the inner membrane by *C. glutamicum* transporters CmpL4 (NCgl0228) and CmpL1 (NCgl2769). The latter has significant sequence similarity to mycobacterial TMM transporter MmpL3, the direct or indirect target of several molecules with antimycobacterial activity (16, 20, 21, 39–41). Deletion of both *NCgl2764* and *tmaT* resulted in a phenotype that was essentially identical to that of the single gene knockout lines, supporting the notion that both proteins act sequentially or on the same step within the same pathway.

In addition to the reduced conversion of hTMCM to h2TDCM in the Δ*NCgl2764* strain, a reduced synthesis of PG and Ala-DAG species and the complete absence of acyl-PG–like lipids were observed. Again, this lipid profile was also observed in our Δ*tmaT* mutant (29) and likely reflects global changes in the synthesis of other cell wall components to compensate for the accumulation of hTMCM/ketoTMCM in the IM and loss of TDCM in the OM. Changes in LM mannan chain length were also detected in the *NCgl2764* mutant but were minor relative to the significant changes in other lipid classes and are probably also a secondary effect.

NCgl2764 and its mycobacterial orthologs are annotated as possible methyltransferases based on sequence similarity with a range of SAM-dependent enzymes. Mutagenesis of two glycine residues equivalent to those in PRMT1 known to bind the methyl donor resulted in loss of NCgl2764 activity. Although these analyses support the annotation of NCgl2764 as a methyltransferase, further studies are needed to confirm enzyme activity. We have been unable to find any evidence that TMCM lipids are methylated in WT bacteria, suggesting that NCgl2764 may be involved in regulating the activity of TmaT. This conclusion is supported by the finding that loss of NCgl2764 phenocopies loss of NCgl2759 (TmaT) and the double knockout line. NCgl2764 could either directly methylate TmaT and/or regulate its function through protein–protein interactions. Protein methylation has been shown to modulate the activity of histones, leading to epigenetic effects through repression or

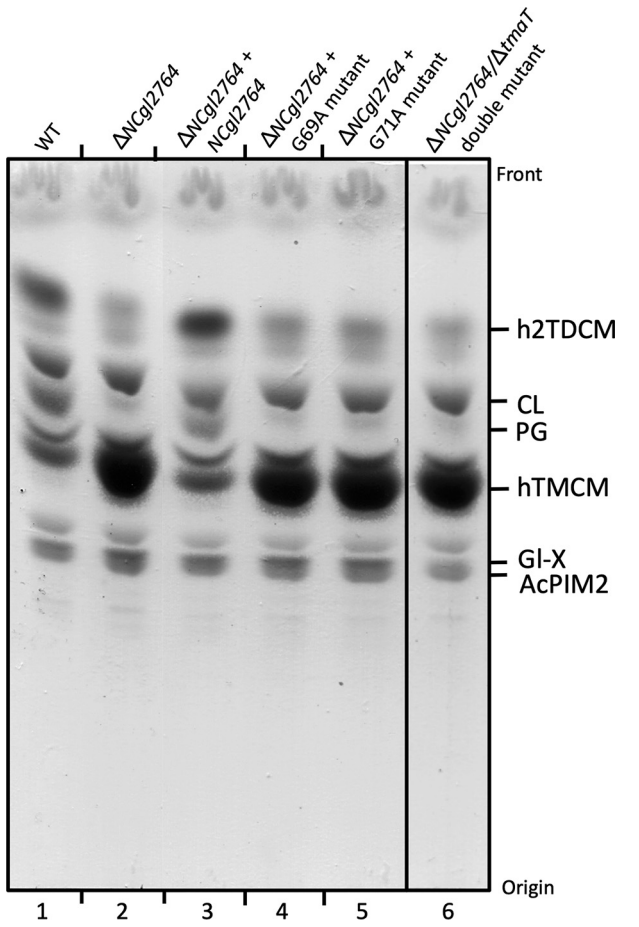

Figure 7. Glycolipid analyses of *NCgl2764* mutants and a Δ*NCgl2764*/Δ*tmaT* double mutant. HPTLC analysis and orcinol/H_2SO_4 staining are shown of glycolipids extracted from WT *C. glutamicum* (*lane 1*), Δ*NCgl2764* (*lane 2*), Δ*NCgl2764* + pSM22:*NCgl2764* (*lane 3*), Δ*NCgl2764* + pSM22:*NCgl2764* carrying G69A substitution (*lane 4*), Δ*NCgl2764* + pSM22:*NCgl2764* carrying G71A substitution (*lane 5*), and a Δ*NCgl2764*/Δ*tmaT* double mutant (*lane 6*).

activation of gene expression (42). Interestingly, histones can also be acetylated (43), and the histone acetyltransferases responsible are themselves often methylated, usually at arginine residues within glycine/arginine-rich "GAR" sequences (44, 45). Alternatively, MtrP and TmaT may form heterodimeric or larger protein complexes. Disruption of one protein could destabilize the other, leading to the similar lipid phenotypes of our mutants. Further studies are required to explore this hypothesis and clarify the relationship between these proteins.

The MtrP ortholog in *M. tuberculosis* H37Rv, Rv0224c, is reported to be essential for *in vitro* growth based on several high-density mutagenesis and sequencing studies (36, 37, 46). Although the cell wall defect in the *NCgl2764* mutant was not reversed by introduction of a plasmid carrying the *Rv0224c* gene, the sequence similarity between the two proteins would suggest that Rv0224c may perform a similar function in this pathogen, making it a potential target for studies aimed at developing new antimycobacterial agents or at making bacterial strains more sensitive to existing agents, a phenotype seen in our mutant.

Experimental procedures

Bacterial strains and culturing conditions

Escherichia coli DH5α was grown in Luria-Bertani (LB) medium at 37 °C with aeration. *C. glutamicum* ATCC 13032 was grown in brain heart infusion (BHI) medium (Oxoid) or LBHIS (LB, BHI, sorbitol) at 30 °C with aeration. When necessary, ampicillin was added to a final concentration of 100 μg ml^{-1} and kanamycin at 50 μg ml^{-1}.

Genetic manipulation of bacteria

E. coli plasmid DNA was isolated using the High Pure plasmid isolation kit (Roche Applied Science), and *C. glutamicum* genomic DNA was extracted using the Illustra DNA extraction kit (GE Healthcare), according to the manufacturer's instructions. DNA manipulations and molecular biology techniques were performed as described (28).

Bioinformatic identification and analysis of NCgl2764

The corynebacterial ortholog of *M. tuberculosis* Rv0224c was found using the BLASTp (47) algorithm. Mycobacterial DNA and protein sequences were obtained from Mycobrowser (RRID:SCR_018242). Amino acid sequence alignments were generated using Clustal Omega (RRID:SCR_001591).

Construction of C. glutamicum ΔNCgl2764 and a ΔNCgl2764/ΔtmaT double mutant

The *NCgl2764* gene was deleted in WT *C. glutamicum* using a two-step allelic replacement strategy (15, 25, 28, 30, 31). A 0.9-kb fragment-containing sequence from the left side of the *NCgl2764* gene was amplified using ProofStart DNA polymerase (Qiagen) with primers NCgl2764leftfor (5′-CCATCCCGGGAAGAACGCCGTGGCGCATCC) and NCgl2764leftrev (5′-CGTATCTAGAGTCAGGTCGGGTTTGTTCGT) and cloned into the SmaI/XbaI sites (underlined) of pUC18 (48), creating plasmid pUC-*NCgl2764*left. A 0.9-kb fragment containing sequence from the right side of *NCgl2764* was amplified using primers NCgl2764rightfor (5′-AATGTCTAGATGGTTGCCGCTTTTCCCCGC) and NCgl2764rightrev (5′-CGACAAGCTTGCTGCTCACCCTAACTCCCG) and cloned into the XbaI/HindIII sites (underlined) of pUC18, creating plasmid pUC-*NCgl2764*right. The right flanking sequence was then excised from pUC-*NCgl2764*right using XbaI/HindIII and subcloned into Xba/HindIII-digested pUC-*NCgl2764*left, fusing the left and right flanking sequences to create plasmid pUC-Δ*NCgl2764*. The 1.8-kb fused insert was then liberated using SmaI/HindIII and subcloned into SmaI/HindIII-digested pK18*mobsacB*, a suicide plasmid for *C. glutamicum* (49) that contains kanamycin and sucrose selection markers. The resultant plasmid, pK18*mobsacB*:Δ*NCgl2764*, was sequenced and then electroporated into electrocompetent *C. glutamicum* cells, prepared as described previously (50), using an ECM 630 electroporator (BTX). Clones resulting from single homologous recombination events were selected on kanamycin. These were grown overnight without antibiotic selection, then serially diluted, and plated onto BHI plates supplemented with 10% (w/v) sucrose to select for a second crossover event. Potential gene knockout mutants (sucrose-resistant, kanamycin-sen-

sitive) were screened by PCR. A Δ*NCgl2764/*Δ*tmaT* double mutant was produced by applying the same approach in an existing Δ*tmaT* mutant strain (28).

Complementation of ΔNCgl2764

To complement the Δ*NCgl2764* strain with the *NCgl2764* gene, a 0.9-kb fragment was PCR-amplified using primers NCgl2764-comp_F (5′-GCGTCTAGATGCCATCACCACCATTTTGC) and NCgl2764-comp_R (5′-CGCTCTAGAGAGCCTTTCTTGTCGTTAAGC), digested with XbaI (underlined), and cloned into the unique PvuII site of pSM22 (32), which contains the corynebacterial origin of replication *repA* and kanamycin resistance gene *aphA3.* To complement the Δ*NCgl2764* strain with the *Rv0224c* gene from *M. tuberculosis*, a 0.9-kb fragment was PCR-amplified using primers Rv0224c_comp-L (5′-TCGGATATCCGATGTCGCGCCAGCACAG) and Rv0224c_comp-R (5′-TCGGATATCGTCATGGCGTCACCCTAC), digested with EcoRV (underlined), and cloned into the unique PvuII site of pSM22. Sequenced complementation plasmids pSM22:*NCgl2764*, pSM22:*Rv0224c*, and an empty pSM22 control plasmid were electroporated into the *C. glutamicum* Δ*NCgl2764* deletion strain, followed by selection on kanamycin-supplemented BHI plates.

Site-directed mutagenesis

Point mutations were introduced into *NCgl2764* using the QuikChange site-directed mutagenesis kit (Stratagene) according to the manufacturer's instructions. The G69A mutation (underlined) was produced using primers A (5′-CTCGACGTCGCCGGCGGACCCGGATACTTCGCC; forward primer) and B (5′-CCGGGTCCGCCGGCGACGTCGAGAACTTTCAGG; reverse primer). The G71A mutation (underlined) was produced using primers C (5′-CGACGTCGGCGGCGCACCCGGATACTTCGCC; forward primer) and D (5′-CGAAGTATCCGGGTGCGCCGCCGACGTCGAGAACTTTC; reverse primer).

Extraction of cell wall components and HPTLC

C. glutamicum strains were grown to logarithmic phase ($OD_{600\ nm}$ = 5–7) or stationary phase ($OD_{600\ nm}$ = 10) in BHI medium (Oxoid). Total lipids were extracted in chloroform/methanol (2:1, v/v) and chloroform/methanol/water (1:2:0.8, v/v) (28). After removal of insoluble material by centrifugation (15,000 × *g*, 10 min), extracts were dried under nitrogen and subjected to biphasic partitioning in 1-butanol and water (2:1, v/v). The organic phase was dried, and lipids were resuspended in 1-butanol. Lipid fractions were analyzed by HPTLC using aluminum-backed silica-gel sheets (Merck). One-dimensional HPTLCs were developed in chloroform, methanol, 13 M ammonium solution, 1 M ammonium acetate, water (180:140:9:9:23, v/v). Glycolipids were stained and visualized with orcinol/H_2SO_4.

Extraction of covalently-bound corynomycolates

Dried, delipidated cell pellets were base-treated to cleave AG-bound corynomycolates. Pellets were suspended in 2 ml of 0.1 M KOH in ethanol (30 °C, 3 h), and samples were neutralized with 0.5 M acetic acid prior to centrifugation at 3000 × *g* for 10 min. Cell pellets were dried by evaporation using a Savant SpeedVac Plus SC11A concentrator and then resuspended by sonication in 400 μl of water-saturated 1-butanol, and mycolates were recovered after phase partitioning in 1-butanol/water (2:1 v/v) and collection of the upper 1-butanol layer.

Pulse-chase radiolabeling

Bacterial strains were grown in BHI to mid-log phase (OD_{600} ~5) at which time the cells were harvested by a 10-min centrifugation at 13,000 × *g*, washed with HEPES-saline (pH 7.4), re-pelleted, and weighed. Pellets were resuspended in HEPES-saline to 0.25 g per ml and incubated for 5 min. Aliquots (200 μl) were transferred to new tubes, and 2 μCi of [^{14}C]acetate was added to each sample (except for the "cold" control) followed by incubation for 5 min. The "pulse" sample was then collected and harvested by brief centrifugation and resuspension of the pellet in 500 μl of chloroform/methanol (2:1 v/v). The "chase" samples were pelleted, and the medium was replaced with prewarmed BHI, followed by incubation at 30 °C for the designated chase time. Chase samples were collected after 5, 15, 30, and 60 min and harvested by brief centrifugation and resuspension of the pellet in 500 μl of chloroform/methanol (2:1 v/v). Following a 1-h extraction, the supernatants were collected by a 5-min centrifugation at 4000 rpm, and the pellets were further extracted for 1 h with 500 μl of chloroform/methanol/water (1:2:0.8 v/v). The glycolipid-containing supernatants were collected by a 5-min centrifugation at 4000 rpm and dried under a N_2 stream. The samples were then suspended in 200 μl of water-saturated 1-butanol and 100 μl of butanol-saturated water, and the butanol phase was collected and dried after vigorous vortexing. The sample was then suspended in 20 μl of 1-butanol, and 2 μl was applied to a HPTLC plate and developed as described above.

Extraction and analysis of lipoglycans

LM and LAM were extracted and purified as described previously (31), separated by PAGE, and stained using a SilverSnap kit (Pierce). Alternatively, purified LM/LAM was suspended in 10 mM ammonium carbonate/bicarbonate buffer (pH 8.16), and 4 μl was injected by direct infusion into an Agilent 6220 Accurate-Mass TOF–LC/MS system (Agilent Technologies). The run was performed in negative ionization mode, with a mass range of 100–3000 Da. The reference nebulizer was set to 20 p.s.i.g. with a detection window of 100 ppm, a minimum height of 1000 counts, an acquisition rate of 0.63 spectra/s, and an acquisition time of 1589.4 ms/spectrum. The gas temperature was set to 325 °C with a drying gas of 7 liters/min, dual ESI 3500 V, fragmentor 150 V, and skimmer 65 V. The flow rate was set to 0.25 ml/min, and a solvent consisting of 0.1 M formic acid, acetonitrile (1:1, v/v) was used to wash the lines for 25 min. Data were analyzed using MassHunter, and the length of the mannan chain was calculated, assuming the presence of a PI lipid anchor containing C16:1/18:1/16:0 fatty acids. Analyses were performed in triplicate.

Extraction of inner and outer membrane lipids for LC/MS and lipidomics analyses

Inner and outer membrane lipids of *C. glutamicum* were extracted and analyzed as described previously (29). In brief, four replicates of WT *C. glutamicum* and mutant strain were grown to exponential phase ($OD_{600\,nm}$ = 2.5–3) in BHI medium. Cells were harvested by centrifugation. The cell pellet was extracted with water-saturated 1-butanol to selectively remove outer membrane lipids. After another centrifugation step, the same pellet was sequentially extracted in chloroform/methanol (2:1, v/v) and chloroform/methanol/water (1:2:0.8, v/v) to extract the remaining lipids of the inner membrane. Both inner and outer membrane lipids were separated on an Agilent 1290 Infinity Quaternary LC System (Agilent Technologies) using a C18 column (Phenomenex Kinetex, 2.6-μm EVO C18 100A) eluted with an isopropyl alcohol mobile phase binary solvent system at a flow rate of 260 μl/min. Eluted lipids were analyzed on a 6550 iFunnel Q-TOF–LC/MS instrument (Agilent Technologies) in positive ionization mode. Lipids were identified based on their *m/z* and fragmentation pattern using a lipid library (29). Statistical analyses were performed using MetaboAnalyst.

Data availability

Data described in this paper are available from the corresponding author upon request (paul.crellin@monash.edu).

Author contributions—A. K. R., S. K., M. J. M., R. L. C., and P. K. C. conceptualization; A. K. R., S. K., Y. Y.-B., R. B., M. J. M., and P. K. C. data curation; A. K. R., S. K., Y. Y.-B., M. J. M., R. L. C., and P. K. C. formal analysis; A. K. R., S. K., Y. Y.-B., R. B., M. J. M., R. L. C., and P. K. C. investigation; A. K. R., S. K., R. B., M. J. M., R. L. C., and P. K. C. methodology; A. K. R., S. K., and P. K. C. writing-original draft; S. K., M. J. M., R. L. C., and P. K. C. validation; S. K., R. L. C., and P. K. C. visualization; M. J. M., R. L. C., and P. K. C. supervision; M. J. M., R. L. C., and P. K. C. funding acquisition; M. J. M., R. L. C., and P. K. C. project administration; M. J. M., R. L. C., and P. K. C. writing-review and editing; R. L. C. resources.

References

1. World Health Organization. (2018) Global Tuberculosis Report 2018, World Health Organization, Geneva, Switzerland
2. Brennan, P. J., and Nikaido, H. (1995) The envelope of mycobacteria. *Annu. Rev. Biochem.* **64,** 29–63 CrossRef Medline
3. Jankute, M., Cox, J. A., Harrison, J., and Besra, G. S. (2015) Assembly of the mycobacterial cell wall. *Annu. Rev. Microbiol.* **69,** 405–423 CrossRef Medline
4. Barry, C. E., 3rd., Lee, R. E., Mdluli, K., Sampson, A. E., Schroeder, B. G., Slayden, R. A., and Yuan, Y. (1998) Mycolic acids: structure, biosynthesis and physiological functions. *Prog. Lipid Res.* **37,** 143–179 CrossRef Medline
5. Daffé, M., and Draper, P. (1998) The envelope layers of mycobacteria with reference to their pathogenicity. *Adv. Microb. Physiol.* **39,** 131–203 CrossRef Medline
6. Hattori, Y., Matsunaga, I., Komori, T., Urakawa, T., Nakamura, T., Fujiwara, N., Hiromatsu, K., Harashima, H., and Sugita, M. (2011) Glycerol monomycolate, a latent tuberculosis-associated mycobacterial lipid, induces eosinophilic hypersensitivity responses in guinea pigs. *Biochem. Biophys. Res. Commun.* **409,** 304–307 CrossRef Medline
7. Druszczynska, M., Kowalski, K., Wawrocki, S., and Fol, M. (2017) Diversity and functionality of mycobacterial mycolic acids in relation to host–pathogen interactions. *Curr. Med. Chem.* **24,** 4267–4278 CrossRef Medline
8. Marrakchi, H., Lanéelle, M. A., and Daffé, M. (2014) Mycolic acids: structures, biosynthesis, and beyond. *Chem. Biol.* **21,** 67–85 CrossRef Medline
9. Raman, K., Rajagopalan, P., and Chandra, N. (2005) Flux balance analysis of mycolic acid pathway: targets for anti-tubercular drugs. *PLoS Comput. Biol.* **1,** e46 CrossRef Medline
10. Takayama, K., Wang, C., and Besra, G. S. (2005) Pathway to synthesis and processing of mycolic acids in *Mycobacterium tuberculosis*. *Clin. Microbiol. Rev.* **18,** 81–101 CrossRef Medline
11. Alsayed, S. S. R., Beh, C. C., Foster, N. R., Payne, A. D., Yu, Y., and Gunosewoyo, H. (2019) Kinase targets for mycolic acid biosynthesis in *Mycobacterium tuberculosis*. *Curr. Mol. Pharmacol.* **12,** 27–49 CrossRef Medline
12. Fernandes, N. D., and Kolattukudy, P. E. (1996) Cloning, sequencing and characterization of a fatty acid synthase-encoding gene from *Mycobacterium tuberculosis* var. *bovis* BCG. *Gene* **170,** 95–99 CrossRef Medline
13. Bhatt, A., Molle, V., Besra, G. S., Jacobs, W. R., Jr., and Kremer, L. (2007) The *Mycobacterium tuberculosis* FAS-II condensing enzymes: their role in mycolic acid biosynthesis, acid-fastness, pathogenesis and in future drug development. *Mol. Microbiol.* **64,** 1442–1454 CrossRef Medline
14. Portevin, D., De Sousa-D'Auria, C., Houssin, C., Grimaldi, C., Chami, M., Daffé, M., and Guilhot, C. (2004) A polyketide synthase catalyzes the last condensation step of mycolic acid biosynthesis in mycobacteria and related organisms. *Proc. Natl. Acad. Sci. U.S.A.* **101,** 314–319 CrossRef Medline
15. Lea-Smith, D. J., Pyke, J. S., Tull, D., McConville, M. J., Coppel, R. L., and Crellin, P. K. (2007) The reductase that catalyzes mycolic motif synthesis is required for efficient attachment of mycolic acids to arabinogalactan. *J. Biol. Chem.* **282,** 11000–11008 CrossRef Medline
16. Xu, Z., Meshcheryakov, V. A., Poce, G., and Chng, S. S. (2017) MmpL3 is the flippase for mycolic acids in mycobacteria. *Proc. Natl. Acad. Sci. U.S.A.* **114,** 7993–7998 CrossRef Medline
17. Su, C. C., Klenotic, P. A., Bolla, J. R., Purdy, G. E., Robinson, C. V., and Yu, E. W. (2019) MmpL3 is a lipid transporter that binds trehalose monomycolate and phosphatidylethanolamine. *Proc. Natl. Acad. Sci. U.S.A.* **116,** 11241–11246 CrossRef Medline
18. Li, W., Stevens, C. M., Pandya, A. N., Darzynkiewicz, Z., Bhattarai, P., Tong, W., Gonzalez-Juarrero, M., North, E. J., Zgurskaya, H. I., and Jackson, M. (2019) Direct inhibition of MmpL3 by novel antitubercular compounds. *ACS Infect. Dis.* **5,** 1001–1012 CrossRef Medline
19. Williams, J. T., Haiderer, E. R., Coulson, G. B., Conner, K. N., Ellsworth, E., Chen, C., Alvarez-Cabrera, N., Li, W., Jackson, M., Dick, T., and Abramovitch, R. B. (2019) Identification of new MmpL3 inhibitors by untargeted and targeted mutant screens defines MmpL3 domains with differential resistance. *Antimicrob. Agents Chemother.* **63,** e00547-19 CrossRef Medline
20. Li, W., Upadhyay, A., Fontes, F. L., North, E. J., Wang, Y., Crans, D. C., Grzegorzewicz, A. E., Jones, V., Franzblau, S. G., Lee, R. E., Crick, D. C., and Jackson, M. (2014) Novel insights into the mechanism of inhibition of MmpL3, a target of multiple pharmacophores in *Mycobacterium tuberculosis*. *Antimicrob. Agents Chemother.* **58,** 6413–6423 CrossRef Medline
21. Dupont, C., Chen, Y., Xu, Z., Roquet-Banères, F., Blaise, M., Witt, A. K., Dubar, F., Biot, C., Guérardel, Y., Maurer, F. P., Chng, S. S., and Kremer, L. (2019) A piperidinol-containing molecule is active against *Mycobacterium tuberculosis* by inhibiting the mycolic acid flippase activity of MmpL3. *J. Biol. Chem.* **294,** 17512–17523 CrossRef Medline
22. Belisle, J. T., Vissa, V. D., Sievert, T., Takayama, K., Brennan, P. J., and Besra, G. S. (1997) Role of the major antigen of *Mycobacterium tuberculosis* in cell wall biogenesis. *Science* **276,** 1420–1422 CrossRef Medline
23. Alderwick, L. J., Radmacher, E., Seidel, M., Gande, R., Hitchen, P. G., Morris, H. R., Dell, A., Sahm, H., Eggeling, L., and Besra, G. S. (2005) Deletion of Cg-emb in Corynebacterianeae leads to a novel truncated cell wall arabinogalactan, whereas inactivation of Cg-ubiA results in an arabinan-deficient mutant with a cell wall galactan core. *J. Biol. Chem.* **280,** 32362–32371 CrossRef Medline
24. Alderwick, L. J., Seidel, M., Sahm, H., Besra, G. S., and Eggeling, L. (2006) Identification of a novel arabinofuranosyltransferase (AftA) involved in

cell wall arabinan biosynthesis in *Mycobacterium tuberculosis*. *J. Biol. Chem.* **281,** 15653–15661 CrossRef Medline

25. Lea-Smith, D. J., Martin, K. L., Pyke, J. S., Tull, D., McConville, M. J., Coppel, R. L., and Crellin, P. K. (2008) Analysis of a new mannosyltransferase required for the synthesis of phosphatidylinositol mannosides and lipoarbinomannan reveals two lipomannan pools in Corynebacterineae. *J. Biol. Chem.* **283,** 6773–6782 CrossRef Medline
26. Mishra, A. K., Alderwick, L. J., Rittmann, D., Tatituri, R. V., Nigou, J., Gilleron, M., Eggeling, L., and Besra, G. S. (2007) Identification of an $\alpha(1\rightarrow6)$ mannopyranosyltransferase (MptA), involved in *Corynebacterium glutamicum* lipomannan biosynthesis, and identification of its orthologue in *Mycobacterium tuberculosis*. *Mol. Microbiol.* **65,** 1503–1517 CrossRef Medline
27. Mishra, A. K., Alderwick, L. J., Rittmann, D., Wang, C., Bhatt, A., Jacobs, W. R., Jr., Takayama, K., Eggeling, L., and Besra, G. S. (2008) Identification of a novel $\alpha(1\rightarrow6)$ mannopyranosyltransferase MptB from *Corynebacterium glutamicum* by deletion of a conserved gene, NCgl1505, affords a lipomannan- and lipoarabinomannan-deficient mutant. *Mol. Microbiol.* **68,** 1595–1613 CrossRef Medline
28. Yamaryo-Botte, Y., Rainczuk, A. K., Lea-Smith, D. J., Brammananth, R., van der Peet, P. L., Meikle, P., Ralton, J. E., Rupasinghe, T. W., Williams, S. J., Coppel, R. L., Crellin, P. K., and McConville, M. J. (2015) Acetylation of trehalose mycolates is required for efficient MmpL-mediated membrane transport in Corynebacterineae. *ACS Chem. Biol.* **10,** 734–746 CrossRef Medline
29. Klatt, S., Brammananth, R., O'Callaghan, S., Kouremenos, K. A., Tull, D., Crellin, P. K., Coppel, R. L., and McConville, M. J. (2018) Identification of novel lipid modifications and intermembrane dynamics in *Corynebacterium glutamicum* using high-resolution mass spectrometry. *J. Lipid Res.* **59,** 1190–1204 CrossRef Medline
30. Rainczuk, A. K., Yamaryo-Botte, Y., Brammananth, R., Stinear, T. P., Seemann, T., Coppel, R. L., McConville, M. J., and Crellin, P. K. (2012) The lipoprotein LpqW is essential for the mannosylation of periplasmic glycolipids in Corynebacteria. *J. Biol. Chem.* **287,** 42726–42738 CrossRef Medline
31. Cashmore, T. J., Klatt, S., Yamaryo-Botte, Y., Brammananth, R., Rainczuk, A. K., McConville, M. J., Crellin, P. K., and Coppel, R. L. (2017) Identification of a membrane protein required for lipomannan maturation and lipoarabinomannan synthesis in Corynebacterineae. *J. Biol. Chem.* **292,** 4976–4986 CrossRef Medline
32. McKean, S., Davies, J., and Moore, R. (2005) Identification of macrophage induced genes of *Corynebacterium pseudotuberculosis* by differential fluorescence induction. *Microbes Infect.* **7,** 1352–1363 CrossRef Medline
33. Liao, H. W., Hsu, J. M., Xia, W., Wang, H. L., Wang, Y. N., Chang, W. C., Arold, S. T., Chou, C. K., Tsou, P. H., Yamaguchi, H., Fang, Y. F., Lee, H. J., Lee, H. H., Tai, S. K., Yang, M. H., *et al.* (2015) PRMT1-mediated methylation of the EGF receptor regulates signaling and cetuximab response. *J. Clin. Invest.* **125,** 4529–4543 CrossRef Medline
34. Keller, J. P., Smith, P. M., Benach, J., Christendat, D., deTitta, G. T., and Hunt, J. F. (2002) The crystal structure of MT0146/CbiT suggests that the putative precorrin-8w decarboxylase is a methyltransferase. *Structure* **10,** 1475–1487 CrossRef Medline
35. Zhang, X., and Cheng, X. (2003) Structure of the predominant protein arginine methyltransferase PRMT1 and analysis of its binding to substrate peptides. *Structure* **11,** 509–520 CrossRef Medline
36. Griffin, J. E., Gawronski, J. D., Dejesus, M. A., Ioerger, T. R., Akerley, B. J., and Sassetti, C. M. (2011) High-resolution phenotypic profiling defines genes essential for mycobacterial growth and cholesterol catabolism. *PLoS Pathog.* **7,** e1002251 CrossRef Medline
37. Sassetti, C. M., Boyd, D. H., and Rubin, E. J. (2003) Genes required for mycobacterial growth defined by high density mutagenesis. *Mol. Microbiol.* **48,** 77–84 CrossRef Medline
38. Belardinelli, J. M., Stevens, C. M., Li, W., Tan, Y. Z., Jones, V., Mancia, F., Zgurskaya, H. I., and Jackson, M. (2019) The MmpL3 interactome reveals a complex crosstalk between cell envelope biosynthesis and cell elongation and division in mycobacteria. *Sci. Rep.* **9,** 10728 CrossRef Medline
39. Grzegorzewicz, A. E., Pham, H., Gundi, V. A., Scherman, M. S., North, E. J., Hess, T., Jones, V., Gruppo, V., Born, S. E., Korduláková, J., Chavadi, S. S., Morisseau, C., Lenaerts, A. J., Lee, R. E., McNeil, M. R., and Jackson, M. (2012) Inhibition of mycolic acid transport across the *Mycobacterium tuberculosis* plasma membrane. *Nat. Chem. Biol.* **8,** 334–341 CrossRef Medline
40. La Rosa, V., Poce, G., Canseco, J. O., Buroni, S., Pasca, M. R., Biava, M., Raju, R. M., Porretta, G. C., Alfonso, S., Battilocchio, C., Javid, B., Sorrentino, F., Ioerger, T. R., Sacchettini, J. C., Manetti, F., *et al.* (2012) MmpL3 is the cellular target of the antitubercular pyrrole derivative BM212. *Antimicrob. Agents Chemother.* **56,** 324–331 CrossRef Medline
41. Tahlan, K., Wilson, R., Kastrinsky, D. B., Arora, K., Nair, V., Fischer, E., Barnes, S. W., Walker, J. R., Alland, D., Barry, C. E., 3rd., and Boshoff, H. I. (2012) SQ109 targets MmpL3, a membrane transporter of trehalose monomycolate involved in mycolic acid donation to the cell wall core of *Mycobacterium tuberculosis*. *Antimicrob. Agents Chemother.* **56,** 1797–1809 CrossRef Medline
42. Nakayama, J., Rice, J. C., Strahl, B. D., Allis, C. D., and Grewal, S. I. (2001) Role of histone H3 lysine 9 methylation in epigenetic control of heterochromatin assembly. *Science* **292,** 110–113 CrossRef Medline
43. Verdone, L., Agricola, E., Caserta, M., and Di Mauro, E. (2006) Histone acetylation in gene regulation. *Brief. Funct. Genomic Proteomic* **5,** 209–221 CrossRef Medline
44. McBride, A. E., and Silver, P. A. (2001) State of the Arg: protein methylation at arginine comes of age. *Cell* **106,** 5–8 CrossRef Medline
45. Thandapani, P., O'Connor, T. R., Bailey, T. L., and Richard, S. (2013) Defining the RGG/RG motif. *Mol. Cell* **50,** 613–623 CrossRef Medline
46. DeJesus, M. A., Gerrick, E. R., Xu, W., Park, S. W., Long, J. E., Boutte, C. C., Rubin, E. J., Schnappinger, D., Ehrt, S., Fortune, S. M., Sassetti, C. M., and Ioerger, T. R. (2017) Comprehensive essentiality analysis of the *Mycobacterium tuberculosis* genome via saturating transposon mutagenesis. *mBio* **8,** e02133-16 CrossRef Medline
47. Altschul, S. F., Gish, W., Miller, W., Myers, E. W., and Lipman, D. J. (1990) Basic local alignment search tool. *J. Mol. Biol.* **215,** 403–410 CrossRef Medline
48. Yanisch-Perron, C., Vieira, J., and Messing, J. (1985) Improved M13 phage cloning vectors and host strains: nucleotide sequences of the M13mp18 and pUC19 vectors. *Gene* **33,** 103–119 CrossRef Medline
49. Schäfer, A., Tauch, A., Jäger, W., Kalinowski, J., Thierbach, G., and Pühler, A. (1994) Small mobilizable multi-purpose cloning vectors derived from the *Escherichia coli* plasmids pK18 and pK19: selection of defined deletions in the chromosome of *Corynebacterium glutamicum*. *Gene* **145,** 69–73 CrossRef Medline
50. van der Rest, M. E., Lange, C., and Molenaar, D. (1999) A heat shock following electroporation induces highly efficient transformation of *Corynebacterium glutamicum* with xenogeneic plasmid DNA. *Appl. Microbiol. Biotechnol.* **52,** 541–545 CrossRef Medline